

1 **Breaking the window of detection: Using multi-scale solute tracer studies to assess mass**  
2 **recovery at the detection limit**

3  
4 *This manuscript has been submitted for publication in Water Resources Research. Please note that this*  
5 *version has not undergone peer review and has not been formally accepted for publication. Subsequent*  
6 *version of this manuscript may have slightly different content. If accepted, the final version of this*  
7 *manuscript will be available via the Peer Reviewed Publication DOI link on the right-hand side of this*  
8 *webpage. Please contact the corresponding author with any questions or concerns.*

9  
10 Adam S. Ward<sup>1,2</sup>

11 Steven M. Wondzell<sup>3</sup>

12 Michael N. Gooseff<sup>4</sup>

13 Tim Covino<sup>5</sup>

14 Skuyler Herzog<sup>1,6</sup>

15 Brian McGlynn<sup>7</sup>

16 Robert A. Payn<sup>8</sup>

- 17  
18 1. O'Neill School of Public and Environmental Affairs, Indiana University, Bloomington,  
19 IN, USA  
20 2. Dept. of Biological and Ecological Engineering, Oregon State University, Corvallis, OR,  
21 USA  
22 3. Pacific Northwest Research Station, Forest Service, United States Department of  
23 Agriculture  
24 4. Institute of Arctic and Alpine Research, University of Colorado, Boulder, Colorado, USA  
25 5. Department of Ecosystem Science and Sustainability, Colorado State University, Fort  
26 Collins, CO, USA  
27 6. Natural Resources Program, Oregon State University - Cascades, Bend, OR, USA  
28 7. Division of Earth and Ocean Science, Nicholas School of Environment, Duke University,  
29 Durham, NC, USA  
30 8. Department of Land Resources and Environmental Sciences, Montana State University,  
31 Bozeman, MT, USA  
32

33 Corresponding Author:

34 Adam S. Ward

35 Dept. of Biological and Ecological Engineering

36 Oregon State University

37 116 Gilmore hall

38 124 SW 24<sup>th</sup> St.

39 Corvallis, OR 97331

40  
41 Email: adam.ward@oregonstate.edu

42 Phone: 541-737-2041

43  
44 **Key words:** hyporheic exchange, transit time, river corridor, solute tracer, stream, turnover

45 **Abstract**

46 Stream solute tracers are commonly injected to assess transport and transformation in study  
47 reaches, but results are biased toward the shortest and fastest storage locations. While this bias  
48 has been understood for decades, the impact of an experimental constraint on our understanding  
49 has yet to be considered. Here, we ask how different our understanding of reach- and segment-  
50 scale transport would be if our empirical limits were extended. We demonstrate a novel approach  
51 to manipulate experimental conditions and observe mass that is stored at timescales beyond the  
52 traditional reach-scale window of detection. We are able to explain the fate of an average of 26%  
53 of solute tracer mass that would have been considered as ‘lost’ in a traditional study design  
54 across our 14 replicates, extending our detection limits to characterize flowpaths that would have  
55 been previously unmeasured. We demonstrate how this formerly lost mass leads to predicting  
56 lower magnitudes of gross gains and losses in individual reaches, and ultimately show that the  
57 network turnover we infer from solute tracers represents an upper limit on actual, expected  
58 behavior. Finally, we review the evolution of tracer studies and their interpretation including this  
59 approach and provide a proposed future direction to extend empirical studies to not-before-seen  
60 timescales

61

62 **Key points**

- 63 ● By manipulating design, solute tracer studies can be used to assess the fate of solute mass  
64 along flowpaths that would not normally be detected
- 65 ● Extended mass recovery allows us to understand the formerly unknown fate of more than  
66 26% of all lost tracer mass
- 67 ● Accounting for mass recovery beyond the typical window of detection reduced inferred  
68 channel water turnover, changing interpreted spatial sources of gains

69

70

## 71 **1. Introduction**

72 The time that a parcel of water spends in various locations within a river corridor is a master  
73 variable that reflects the integrated effects of physical stores and fluxes and ultimately controls  
74 the biogeochemical processes and functions that are realized during transport. Empirical  
75 evidence of transit times in river corridors most commonly relies upon naturally occurring  
76 tracers to assess relatively long timescales (Cirpka et al., 2007; Gooseff et al., 2003; Lamontagne  
77 & Cook, 2007) and injected solute tracers for shorter timescales (Stream Solute Workshop, 1990;  
78 Ward et al., 2012). Studies using stream solute tracers are widespread in their application, but for  
79 more than 20 years have been known to be biased toward measuring the fastest portion of the  
80 transit time distribution, a limitation inherent to the method (J. W. Harvey et al., 1996; Wagner  
81 & Harvey, 1997). Despite the recognition of this limit, and the fact that the limitation is itself  
82 highly variable as a function of study design (e.g., Schmadel et al., 2016), hydrologists continue  
83 to conduct and interpret solute tracer studies. Any tracer that is released but not recovered (i.e.,  
84 'lost') is attributed to flow that bypasses the monitoring location or transport along flowpaths  
85 longer than can be detected by monitoring equipment. In the latter case, such flowpaths could  
86 range in timescale from incrementally longer than what is detected to infinitely long. The  
87 inherent limits of tracer studies in streams define an arbitrary boundary that separates the tracer  
88 we are able to sense and interpret from the tracer we lose to the 'black box' of longer timescales.  
89 While this demarcation is conceptually understood, we do not understand how this  
90 methodological threshold changes our understanding of transport in stream reaches (i.e.  
91 individual sections of river that are studied in an experiment, typically 10's to 100's of meters;  
92 Frissell et al., 1986). Moreover, when reaches are combined to represent segment (i.e., sections  
93 of a river that are comprised of multiple reaches, typically 100's to 1000's of meters; Frissell et  
94 al., 1986) it is unclear what impact - if any - the study limitations have on our understanding of  
95 transport in river corridors. Here, we ask how the well-documented and broadly acknowledged  
96 limits of solute tracer studies change our understanding at the reach- and segment-scales. In other  
97 words, if we manipulate the observational constraints of solute tracer studies to 'peer into the  
98 black box', characterizing solute transport at timescales that have traditionally been lost to  
99 unknown fates, what would change about our understanding of transport in river corridors?

100  
101 Stream tracer studies have been broadly successful in advancing our understanding of transport  
102 and fate in river corridors. Solute tracer studies underpin early work on mixing in streams and  
103 rivers (Fischer, 1979), and the reach-scale effects of transient storage both in hyporheic zones  
104 (Bencala, 1983; Bencala et al., 1984; Bencala & Walters, 1983; J. W. Harvey & Wagner, 2000;  
105 Jackman et al., 1984) and within stream channels (Briggs et al., 2009; Jackson et al., 2012, 2013;  
106 Ward et al., 2018). Indeed, tracer studies are a critical component of our ability to predict the fate  
107 of nutrients (Alexander et al., 2009; J. Harvey et al., 2019a; Mulholland et al., 2008; Newbold et  
108 al., 1981; Tank et al., 2008), emerging contaminants (Guillet et al., 2019; Keefe et al., 2004;  
109 Lange et al., 2011), heavy metals (Fuller & Harvey, 2000; J. W. Harvey & Fuller, 1998; Larson  
110 et al., 2013), and more broadly to study timescales of storage in river corridors (Haggerty et al.,  
111 2002; Ward, Kurz, et al., 2019a; Worman & Wachniew, 2007). Tracer studies have also been  
112 used assess the impact of dynamic flow regimes (Karwan & Saiers, 2009; Ward et al., 2013;  
113 Ward, Kurz, et al., 2019b) and restoration (Klocker et al., 2009; Knust et al., 2009; Ward et al.,  
114 2018) on reach- and segment-scale functions. Despite their widespread use and interpretation for  
115 a host of problem, all solute tracer studies are limited by their 'window of detection' (WoD), the  
116 longest temporal scale of flowpath that contributes to a measurable concentration in the stream

117 channel (J. W. Harvey et al., 1996; Wagner & Harvey, 1997) (flowpaths A and B; Fig. 1). Solute  
118 tracer that does not return to the stream to be observed, either due to flowpath geometry  
119 (flowpaths C, D; Fig. 1), timescale (flowpaths E, F; Fig. 1), or both (flowpath G, Fig. 1) are  
120 ultimately lost to unknown fates, limiting interpretations to a subset of the known, multi-scale  
121 flowpaths that exist (Herzog et al., 2019; Toth, 1962; Tóth, 1963).

122  
123 While the known limitations and biases of stream solute tracers have been understood for more  
124 than 25 years, it remains unknown if and how this limitation may actually bias our understanding  
125 of transport. These ‘lost’ timescales and flowpaths are understood to be relevant for  
126 biogeochemical function and complete description of transit time distributions, leading scientists  
127 to developing strategies to extrapolate behavior from observed to ‘lost’ timescales. Such  
128 approaches broadly extrapolate observed data to timescales beyond the WoD, assigning  
129 monotonically decreasing probabilities as timescales extend. Put plainly, the most likely assumed  
130 fate for mass that is ‘lost’ during an injection is to travel along flowpaths with timescales  
131 incrementally longer than the WoD. The next most likely fate is to travel along a slightly longer  
132 flowpath, and so on. This conceptualization is consistent with empirical observations that  
133 targeted extremely long tailing (Haggerty et al., 2002; Ninnemann, 2005) and methods used to  
134 extend the tails of solute tracer data (Drummond et al., 2012). This is also consistent with  
135 StorAge Selection approaches to stream tracer transport, where gamma distributions have  
136 successfully represented monotonically decreasing contributions of older water to stream  
137 discharge (Harman et al., 2016; Ward et al., 2019; Ward, Kurz, et al., 2019a). Taken together,  
138 both our empirical studies, strategies to correct empirical data for known limitations, and  
139 process-agnostic approaches to solute tracers all predict that an incremental extension of the  
140 WoD should yield the most significant change in the observed in-stream breakthrough curve and  
141 subsequent interpretations, with decreasing impact as the WoD was further extended.  
142 Importantly, while the above strategies exist as a basis to extrapolate beyond observations, no  
143 empirical evidence exists to document that they are appropriate in describing the fate of tracer  
144 mass beyond the WoD.

145  
146 The WoD is perhaps the most critical variable in our interpretation of solute tracer studies at  
147 individual reaches and our extrapolation to the segment and network scales. The WoD defines a  
148 fundamental partitioning of tracer mass into two categories: recovered and lost mass. The mass  
149 that was recovered within the WoD is interpreted using time series analyses to infer a host of  
150 transport and transient storage processes (e.g., Covino et al., 2010; J. W. Harvey & Wagner,  
151 2000; Newbold et al., 1981; Stream Solute Workshop, 1990). The fate of mass along all other  
152 flowpaths is ultimately unknown. Although the fate of lost mass is empirically unknown, the  
153 magnitude of mass loss is used to interpret reach-scale water balances through gross gains and  
154 losses of channel water within a study reach (i.e., channel water balance; Payn et al., 2009),  
155 which themselves form the basis of how we predict channel water turnover along segments and  
156 river networks (Covino et al., 2011; Mallard et al., 2014). Critical to these analyses are the  
157 magnitude of mass that is ultimately lost, but that partitioning is known to be a function of study  
158 design itself (Schmadel et al., 2016), ultimately reflecting the WoD for the empirical studies. In  
159 this framework, increased mass recovery due to an extended WoD would decrease mass loss,  
160 consequently reducing magnitudes of gross gains and losses, ultimately reducing inferred  
161 channel turnover.

162

163 While the WoD is a well-known limitation of stream solute tracers, it has traditionally been  
164 accepted as a methodological limitation, either described post-hoc or as a basis to standardize  
165 experimental designs (e.g., Ward et al., 2018, 2019). Here, we posit that manipulation of the  
166 WoD may be used to our advantage, specifically enabling us to assess solute transport that is just  
167 beyond the WoD for a common study, assessing the marginal gains in mass recovery - and  
168 understanding - associated with solute tracer mass that is just beyond our detection limits. In this  
169 study, we assess the influence of flowpaths that are incrementally longer than the WoD for a  
170 study reach by comparing the results of stream solute tracer tests in shorter reaches nested within  
171 longer reaches of the same stream. By doing so, we provide the first empirical test of the  
172 expectation that much of the lost tracer mass is being transported along flowpaths that are  
173 marginally longer than the WoD (Drummond et al., 2012; Harman et al., 2016). We term the  
174 added mass that is recovered when the WoD is experimentally extended ‘marginal mass  
175 recovery’. Specific objectives of this study include: (1) empirical documentation ‘marginal mass  
176 recovery’ in a series of study reaches; (2) assessment of how marginal mass recovery changes  
177 interpreted reach-scale channel water balance; and (3) assessment of how marginal mass  
178 recovery changes our interpretation of segment-scale turnover. To achieve these objectives, we  
179 evaluate a series of solute tracer experiments conducted in the same study segment, either as two  
180 sequential 100-m reaches (hereafter 2x100-m) or a single 200-m reach. We derive an ‘extended’  
181 mass balance that accounts for marginal mass recovery and demonstrate the change in  
182 interpretation that results from convolving these observations along a river segment. Finally, we  
183 address the crux of what is to be done with empirically imperfect data and their application to  
184 process understanding and scaling of findings.

185  
186

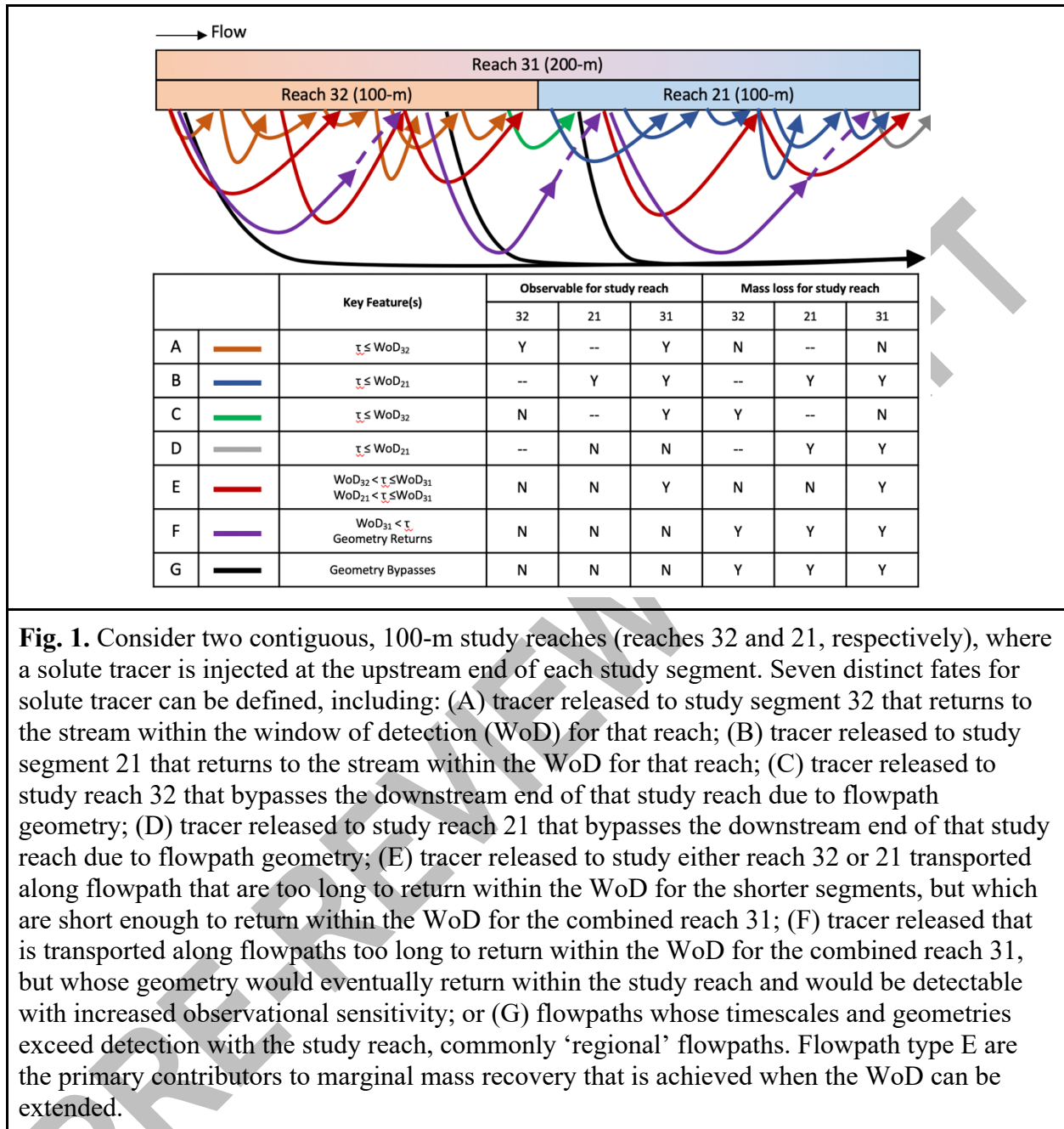


**Fig. 1.** Consider two contiguous, 100-m study reaches (reaches 32 and 21, respectively), where a solute tracer is injected at the upstream end of each study segment. Seven distinct fates for solute tracer can be defined, including: (A) tracer released to study segment 32 that returns to the stream within the window of detection (WoD) for that reach; (B) tracer released to study segment 21 that returns to the stream within the WoD for that reach; (C) tracer released to study reach 32 that bypasses the downstream end of that study reach due to flowpath geometry; (D) tracer released to study reach 21 that bypasses the downstream end of that study reach due to flowpath geometry; (E) tracer released to study either reach 32 or 21 transported along flowpath that are too long to return within the WoD for the shorter segments, but which are short enough to return within the WoD for the combined reach 31; (F) tracer released that is transported along flowpaths too long to return within the WoD for the combined reach 31, but whose geometry would eventually return within the study reach and would be detectable with increased observational sensitivity; or (G) flowpaths whose timescales and geometries exceed detection with the study reach, commonly ‘regional’ flowpaths. Flowpath type E are the primary contributors to marginal mass recovery that is achieved when the WoD can be extended.

188

## 189 2. Methods

### 190 2.1 Study site and field experiment

191 Stringer Creek is a second-order stream in the Tenderfoot Creek Experimental Forest in the Little  
 192 Belt Range of the Rocky Mountains in Montana, United States. The stream drains about 5.5 km<sup>2</sup>  
 193 of primarily forested land. The valley is underlain by granite-gneiss bedrock along the lower  
 194 1600-m of the study, while upper reaches are underlain by sandstone bedrock. The upper valley  
 195 has a generally wider valley floor, lower-relief hillslope, and flatter longitudinal slope than the

196 lower valley. Additional site characteristics can be found in several prior studies (Kelleher et al.,  
197 2013; Patil et al., 2013; Payn et al., 2009; Ward et al., 2016).

198  
199 Our study design divided the river corridor into a series of contiguous 200-m segments. Each  
200 200-m segment was studied with a series of three solute tracer releases at locations 1, 2, and 3  
201 (Fig. 2A). Each injection was monitored at all downstream locations, allowing us to study the  
202 segment as two independent 100-m reaches (i.e., reach 32 and 21), or a single 200-m segment  
203 (i.e., reach 31). Additional details on the experimental design and prior analyses can be found in  
204 several related studies (Kelleher et al., 2013; Patil et al., 2013; Payn et al., 2009; Ward et al.,  
205 2016). Notably, the dataset has been independently analyzed as both 100-m and 200-m reaches,  
206 but the two have yet to be quantitatively compared to learn from deviations between the length  
207 scales and WoDs.

208  
209 First, an injection of a known tracer mass is injected sequentially one mixing length upstream  
210 from each of points 1, 2, and 3. Discharge at each location was calculated by dilution gauging as:  
211

$$212 \quad Q_X = \frac{M_X}{\int_{t=0}^{t=\infty} C_X(t) dt}$$

213  
214 where  $X$  denotes the location number,  $C_X(t)$  is the observed in-stream tracer concentration  
215 at location  $X$  ( $\text{g m}^{-3}$ ),  $M_X$  is the injected solute tracer mass at each location ( $\text{g}$ ), and  $t$  is time  
216 ( $\text{s}$ ). The tracer releases at points 2 and 3 are also recorded as they pass the downstream  
217 loggers, yielding in-stream concentration time series  $C_{21}(t)$ ,  $C_{32}(t)$ , and  $C_{31}(t)$ , where  $C_{XY}$   
218 denotes an injection from location  $X$  observed in-stream at location  $Y$ . The mass recovered  
219 at any location can be calculated as:

$$220 \quad M_{recXY} = Q_Y \int_{t=0}^{t=\infty} C_{XY}(t) dt.$$

221  
222 Mass recovery can also be expressed as a fraction of input mass ( $f_{XY}$ ) as:

$$223 \quad f_{recXY} = \frac{M_{recXY}}{M_X}.$$

224  
225 Total and fractional mass losses ( $M_{LOSSXY}$  and  $f_{lossXY}$ ) can also be calculated as:

$$226 \quad M_{LOSSXY} = M_X - M_{recXY}$$

227  
228 and

$$229 \quad f_{lossXY} = 1 - f_{recXY}$$

## 230 231 232 233 234 235 **2.2 Analysis of lost mass**

### 236 **2.2.1 Channel water balance**

237 Payn et al. (2009) provide a framework to interpret tracer mass losses and calculate reach-  
238 scale gross gains ( $Q_{GAIN}$ ) and gross losses ( $Q_{LOSS}$ ). Briefly, gross losses of stream water are  
239

240 calculated by considering either gain-before-loss (i.e., maximum dilution before loss,  
241 subscript  $MAX$ ):

242

$$243 \quad Q_{LOSS,MAX} = \frac{M_{LOSS,XY}}{\int_{t=0}^{t=\infty} C_{XX}(t)dt}$$

244

245 or loss-before-gain (i.e., minimum dilution before loss, subscript  $MIN$ ):

246

$$247 \quad Q_{LOSS,MIN} = \frac{M_{LOSS,XY}}{\int_{t=0}^{t=\infty} C_{XY}(t)dt}$$

248

249 where  $M_{LOSS}$  is the mass loss along a study reach for an injection at location  $X$  observed in-  
250 stream at location  $Y$ . Next, the net change in discharge ( $\Delta Q$ ) can be calculated as:

251

$$252 \quad \Delta Q = Q_Y - Q_X$$

253

254 Finally, knowledge of the net change in discharge and the gross losses can be used to  
255 calculate gross gains as:

256

$$257 \quad Q_{GAIN,MAX} = \Delta Q - Q_{LOSS,MAX}$$

258

259 and

$$260 \quad Q_{GAIN,MIN} = \Delta Q - Q_{LOSS,MIN}$$

261

262 In this study we proceed with interpretation of the loss-before-gain assumption, which  
263 assumes the minimum turnover of stream water caused by gross gains and losses along the  
264 study reach (after Covino, Ward).

265

### 266 **2.2.2 Network turnover**

267 *Covino et al. (2011)* extended the interpretation of segment-scale channel water balances to  
268 river networks, developing a method to interpret network turnover. Briefly, the discharge in  
269 a downstream segment  $i$  can be calculated as:

270

$$271 \quad Q_i = Q_{i-1} + Q_{GAIN} - Q_{LOSS}$$

272

273 The simultaneous gain and loss of water is assumed to remove water from all upstream  
274 segments equally, causing a volume-weighted replacement of upstream water with newly  
275 inflowing water. This is calculated as:

276

$$277 \quad Q_{i,j} = Q_{i-1,j} \frac{Q_i - Q_{GAIN,i}}{Q_i}$$

278

279 where  $Q_{i,j}$  is the discharge in segment  $i$  contributed by an upstream segment  $j$ ,  $Q_{i-1,j}$  is the  
280 stream water contribution to segment  $i-1$  that entered in segment  $j$ , and the fractional term



281 is the proportional contribution to  $Q_i$  from all upstream segments. This calculation can be  
 282 completed sequentially from the headwaters to downstream end of the study segment. The  
 283 result is an apportionment of the discharge in each study segment to the location(s) where  
 284 that water last entered the stream channel.

285

### 286 **2.3 Analysis of marginal mass recovery**

287 If the two 100-m study segments are assumed to act independently and are combined in  
 288 series to represent the single 200-m segment (Fig. 2C), the mass recovered from the  
 289 combined segment is calculated as the effect of the two segments acting on the upstream  
 290 input in series:

291

292

$$M_{rec31} = M_3 f_{rec32} f_{rec21}$$

293

294 where  $M_{rec31,expected}$  is the expected mass recovery from a slug at location 3 observed at  
 295 location 1 based on the linear convolution of the sub-segments. However, in practice this  
 296 linear combination of segments may not be observed. Instead, studying a longer reach is  
 297 expected to extend the experimental WoD and allow increased mass recovery (i.e.,  
 298  $M_{rec31,extended} > M_{rec31}$ , compare Fig. 2C and 2D). We term the extra mass recovered in the  
 299 longer study segment the marginal mass recovery ( $M_{marg}$ ), calculated as:

300

301

$$M_{marg} = M_{rec31,extended} - M_{rec31}$$

302

303 Conceptually,  $M_{marg}$  represents mass that was stored along flowpaths that were longer than  
 304 could be detected in the observed  $C_{21}$  or  $C_{32}$  but short enough to return to the stream and  
 305 contribute to  $C_{31}$  (i.e., flowpath E in Fig. 1) or flow that bypassed the sensor at location 2  
 306 (i.e., flowpath C in Fig. 1). Put another way, the timescales of intermediate storage ( $t_{int}$ ) may  
 307 be expressed as:

308

309

$$(t_{21}, t_{32}) < t_{int} < t_{31}$$

310

311 where  $t_{XY}$  represents the window of detection for an injection at location  $X$  observed at  
 312 location  $Y$ ). While some marginal mass recovery is associated with flow that bypassed  
 313 location 2 in the subsurface and returned to the stream (flowpath C in Fig. 1), we assume  
 314 this mass is negligible compared to the return of longer flowpaths along the entirety of the  
 315 segment. The mass balance for the system of segments (Fig. 2) can be written as:

316

317

$$M_3 = M_{rec31} + M_{loss32} + M_{loss21}$$

318

319 where  $M_3$  is the mass input for the upstream-most injection. Calculations of masses for each  
 320 individual segment and associated flowpaths are detailed in the supplement to this study.  
 321 Mass losses from the shorter segments can be calculated as:

322

323

$$M_{loss32} = M_3(1 - f_{rec32})(1 - f_{int32})$$

324

325 and

326  
327  
328  
329  
330  
331  
332  
333  
334  
335  
336  
337  
338  
339  
340  
341  
342  
343  
344  
345  
346  
347  
348  
349  
350  
351  
352  
353  
354  
355  
356  
357  
358  
359  
360

$$M_{loss21} = M_3[f_{rec32} + (1 - f_{rec32})f_{int32}](1 - f_{rec21})(1 - f_{int21})$$

Input mass ( $M_3$ ) and recovered mass ( $M_{rec31}$ ) are related by:

$$M_{rec31} = M_3[f_{rec32} + (1 - f_{rec32})f_{int32}][f_{rec21} + (1 - f_{rec21})f_{int21}]$$

(see supplemental material for an extended derivation).

Based on the experimental design (Fig. 2A), values are known for  $M_3$ ,  $M_{rec31}$ ,  $f_{rec32}$ , and  $f_{rec21}$ . The unknowns in the system are  $f_{int32}$  and  $f_{int21}$  which partition segment-by-segment losses into  $M_{marg}$  and  $M_{loss}$  for each study segment. We proceed with the assumption that mass beyond the window of detection in the two 100-m study segments is equally likely to return within the window of detection for the combined, longer segment (i.e.,  $f_{int32}=f_{int21}$ ). Finally, the mass balances for the individual and combined releases can be combined to yield an analytical solution for the system.

With the marginal mass recovery calculated, we next calculate an ‘extended’ mass recovery. This ‘extended’ recovery considers how the 100-m segment would be expected to behave if the WoD were extended to that of the 200-m segment. In other words, this step extends the empirical 100-m data to its expected, marginally longer behavior, accounting for the mass actually recovered (e.g.,  $M_{rec21}$ ) and the marginal mass recovery (e.g.,  $M_{marg21}$ ). Put another way, we can estimate the mass that would have been recovered for a marginally longer window of detection in each 100-m segment as:

$$M_{rec21,extended} = M_{rec21} + M_{marg21}$$

$$M_{rec32,extended} = M_{rec32} + M_{marg32}$$

where  $M_{recXY,extended}$  represents the mass recovery in segment XY that would be realized if the 100-m study had the window of detection associated with the 200-m study. In turn, mass losses, channel water balance, and turnover calculations can be updated using these extended values.

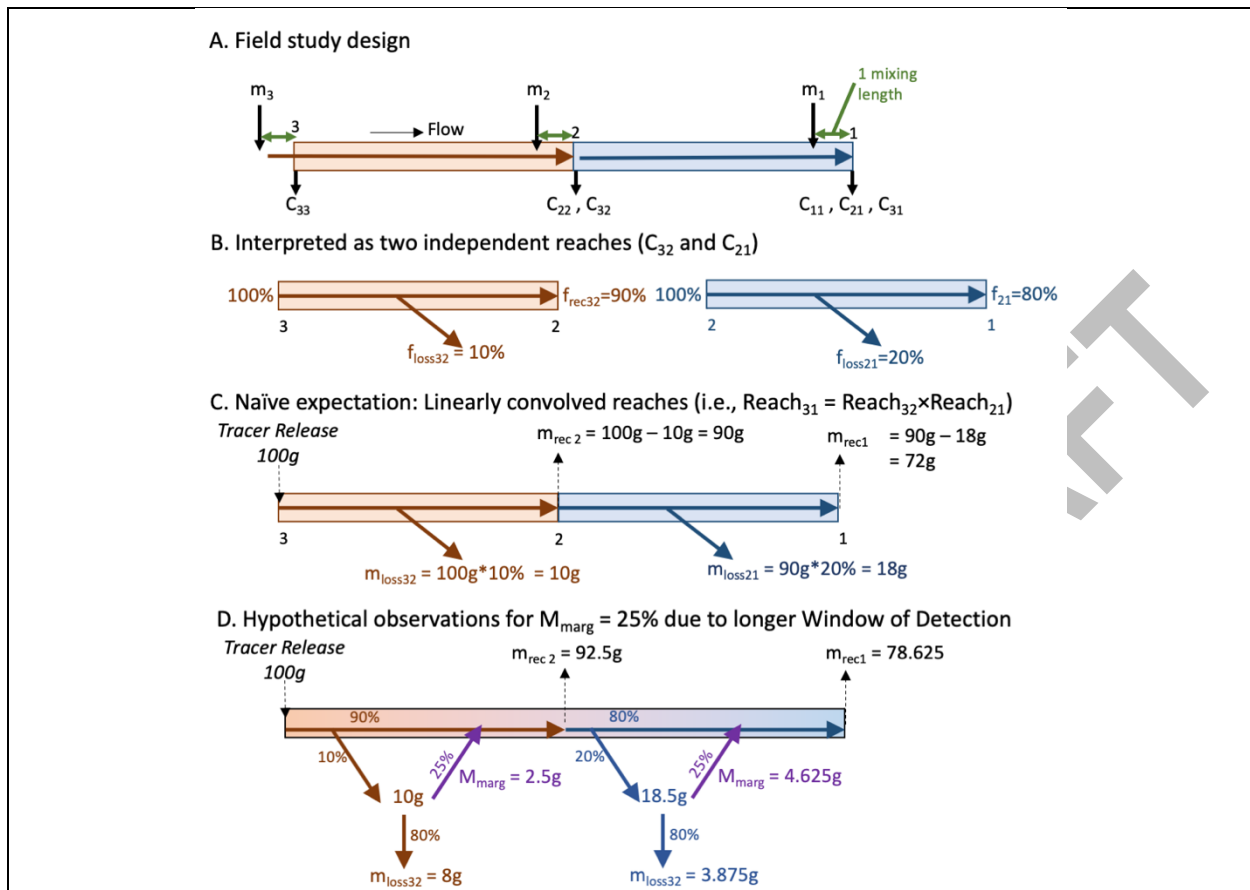


Fig. 2. (A) Field study design showing tracer mass releases ( $m_x$ ) and observed in-stream solute tracer timeseries ( $C_{XY}$ ), where  $X$  is the release location and  $Y$  is the observation location. (B) Partitioning of recovered and lost solute tracer mass for two reaches interpreted independently. (C) Mass losses and recovery for a hypothetical 100-g solute tracer release at the upstream end of the study site, assuming the two 100-m reaches act on the input in series. (D) Mass losses and recovery for a hypothetical 100-g solute tracer release at the upstream end of the study site, assuming that the extended window of detection for a longer study reach yields 25% more mass recovery.

361  
362  
363

### 3. Results

#### 3.1 Marginal mass recovery and channel water balance

364 The fraction of tracer mass loss in 200-m reaches is neither systematically greater nor smaller in  
365 magnitude than their component 100-m reaches (Fig. 3A). However, total mass loss for the  
366 convolved 2x100-m case is always greater than the observed mass loss in each of the 200-m  
367 segments (Fig. 3B). This increased mass recovery indicates some mass that was lost from the  
368 100-m studies was recovered in the 200-m study with its longer WoD, confirming the presence  
369 of marginal mass recovery,  $M_{marg}$ . We found an average of 26.2% of mass presumed to be lost  
370 from the 100-m studies was ultimately recovered in the 200-m study segment (range 6.5-63.1%,  
371 median 20.7%, standard deviation 17.2%; Fig. 4A). These marginal recoveries represent an  
372 average of 4.3% of total tracer mass (range 1.3-10.1%, median 3.4%, standard deviation 2.6%;  
373 Fig. 4A) recovered in the 200-m studies that was lost in the 2x100-m interpretation. Increased  
374 mass recovery yields decreased magnitudes of gross gains and losses for each of the 200-m

375 reaches considered (Fig. 4B). Additionally, gross gains and losses for the extended 100-m  
376 reaches are always lower in magnitude than their empirically observed counterparts, as expected  
377 for  $M_{marg}>0$  (Fig. 4C).  
378

PRE-REVIEW DRAFT

379  
380

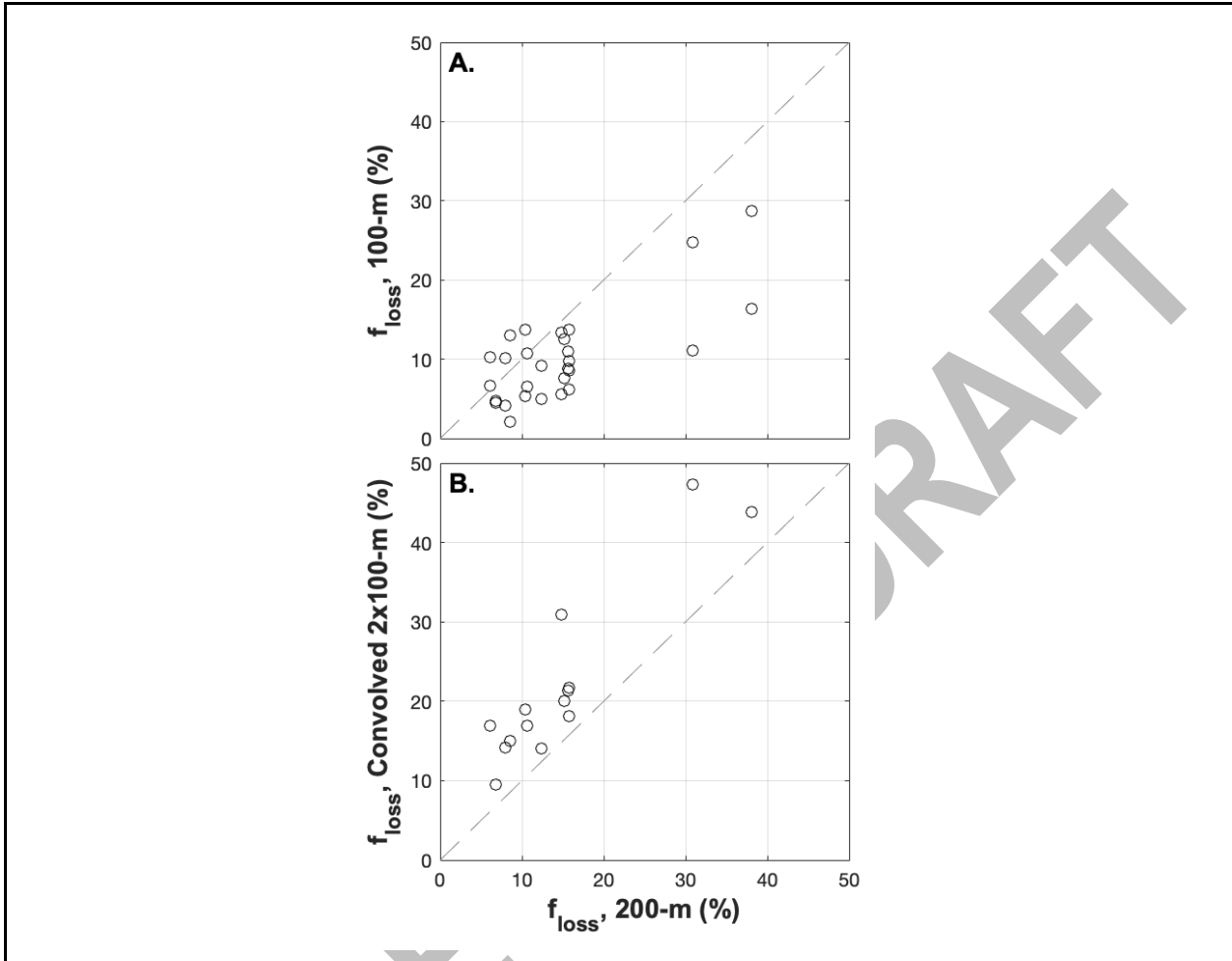


Fig. 3. Comparison of the fraction of injected mass loss ( $f_{loss}$ ) observed for 200-m study reaches (x-axis) in comparison to the same study reach studied as two 100-m reaches considered (A) individually, and (B) convolved in series. The convolution of two 100-m reaches to represent the 200-m overpredicts mass loss in all 14 replicates (i.e., more mass is recovered for the 200-m empirical study that would be expected). This systematic overprediction of losses is the result of marginal mass recovery in the 200-m reach.

381  
382

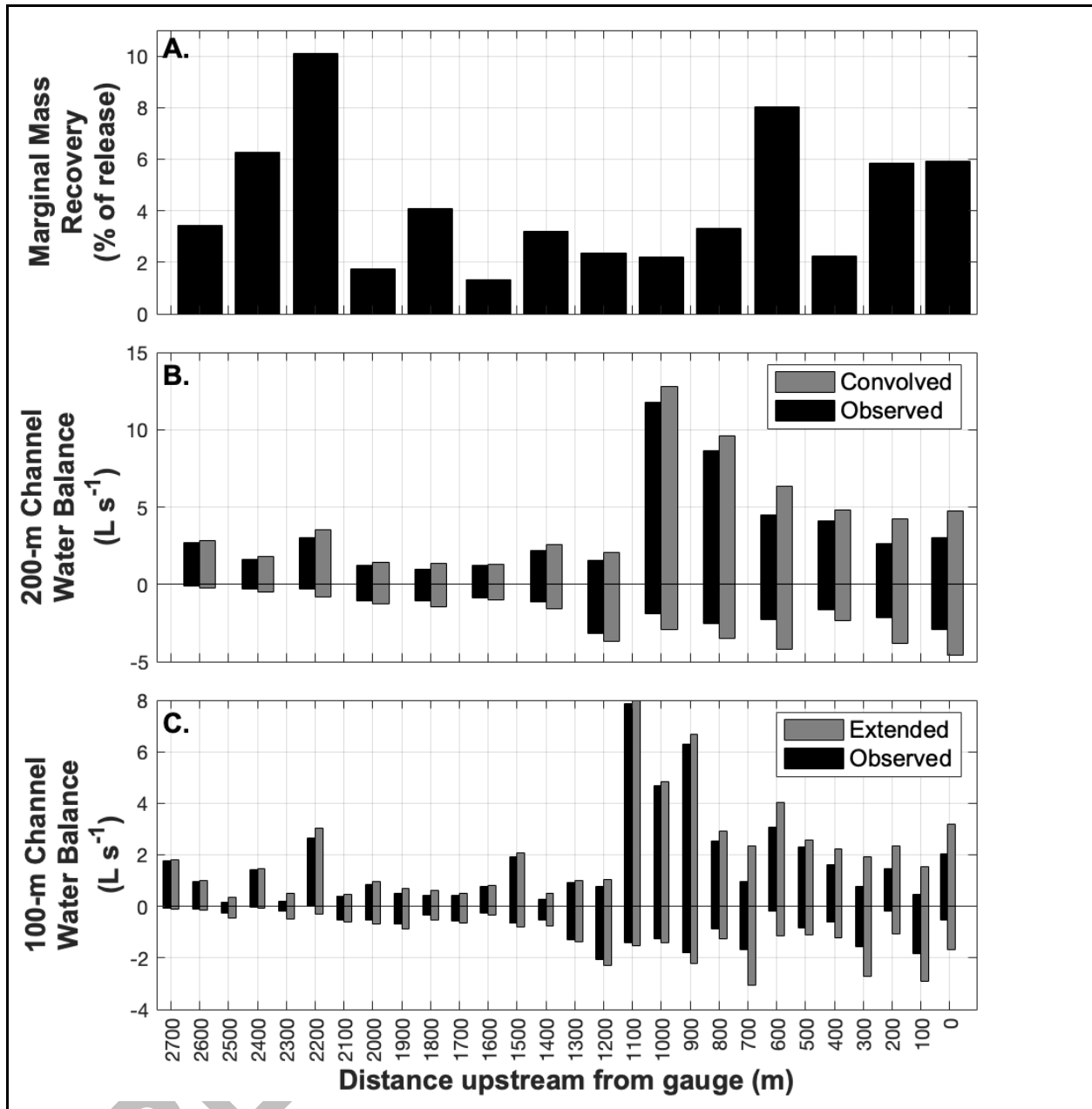


Fig. 4. (A) Magnitude of marginal mass recovery for each 200-m reach compared to its component 100-m reaches, expressed as total percent of tracer. (B) Gross gains (positive bars) and losses (negative bars) for the observed 200-m experiments and what would be expected based on linear convolution of the underlying 100-m reaches. Convolution of two 100-m segments always yields larger magnitudes of gross gains and losses than are inferred from 200-m studies. (C) Gross gains and losses for 100-m segments using the observed and extended mass balance calculations.

383

### 384 3.2 Network turnover

385 The systematic overestimations of  $Q_{LOSS}$  and  $Q_{GAIN}$  in the 100-m reaches are amplified when  
 386 results are aggregated along the study segment to predict stream water turnover. The empirical

387 mass recoveries yield higher magnitudes for  $Q_{LOSS}$  and  $Q_{GAIN}$  in each segment than their  
388 extended counterparts (visible as the differences in heights of individual segments within stacked  
389 bars of Fig. 5A). The result of increased magnitudes is more rapid replacement of upstream  
390 waters by downstream inflows for the empirical data in comparison to the extended values. If  
391 turnover is overpredicted, then predictions of stream water residence time in the channel will be  
392 shorter when compared to extended interpretations, with more outflowing water being attributed  
393 to locations closer to the outlet. This effect accumulates along the full length of the stream  
394 channel, yielding two related patterns. First, the persistence of upstream waters along the  
395 segment is systematically underestimated using empirical data (visible by the preponderance of  
396 upstream, 'bluer' bars below 0 in Figs. 5B,). For example, discharge at the outlet from the  
397 upstream-most segment is calculated as about  $0.03 \text{ L s}^{-1}$  based on empirical observations,  
398 compared to nearly  $0.1 \text{ L s}^{-1}$  based on extended calculations. At the basin outlet, contributions  
399 from the upper 2000-m are underestimated by nearly 50% based on empirical data compared to  
400 the extended interpretation. Next, the overpredicted turnover from empirical data requires that  
401 downstream contributions are overestimated, yielding a systematic overprediction of the  
402 contributions of downstream reaches to the stream water composition (visible by the  
403 preponderance of downstream, 'yellower' bars above 0 in Figs. 5B). For example, at the  
404 downstream end of the study segment (right-most bars in Fig. 5), inflows from the lower 800-m  
405 of the study segment are overestimated at the catchment outlet by about 20%. Thus, while  
406 general patterns of turnover are visually similar (Fig. 5A), the expected composition of the water  
407 in the stream is quite different (Fig. 5B) between empirical and extended cases.  
408

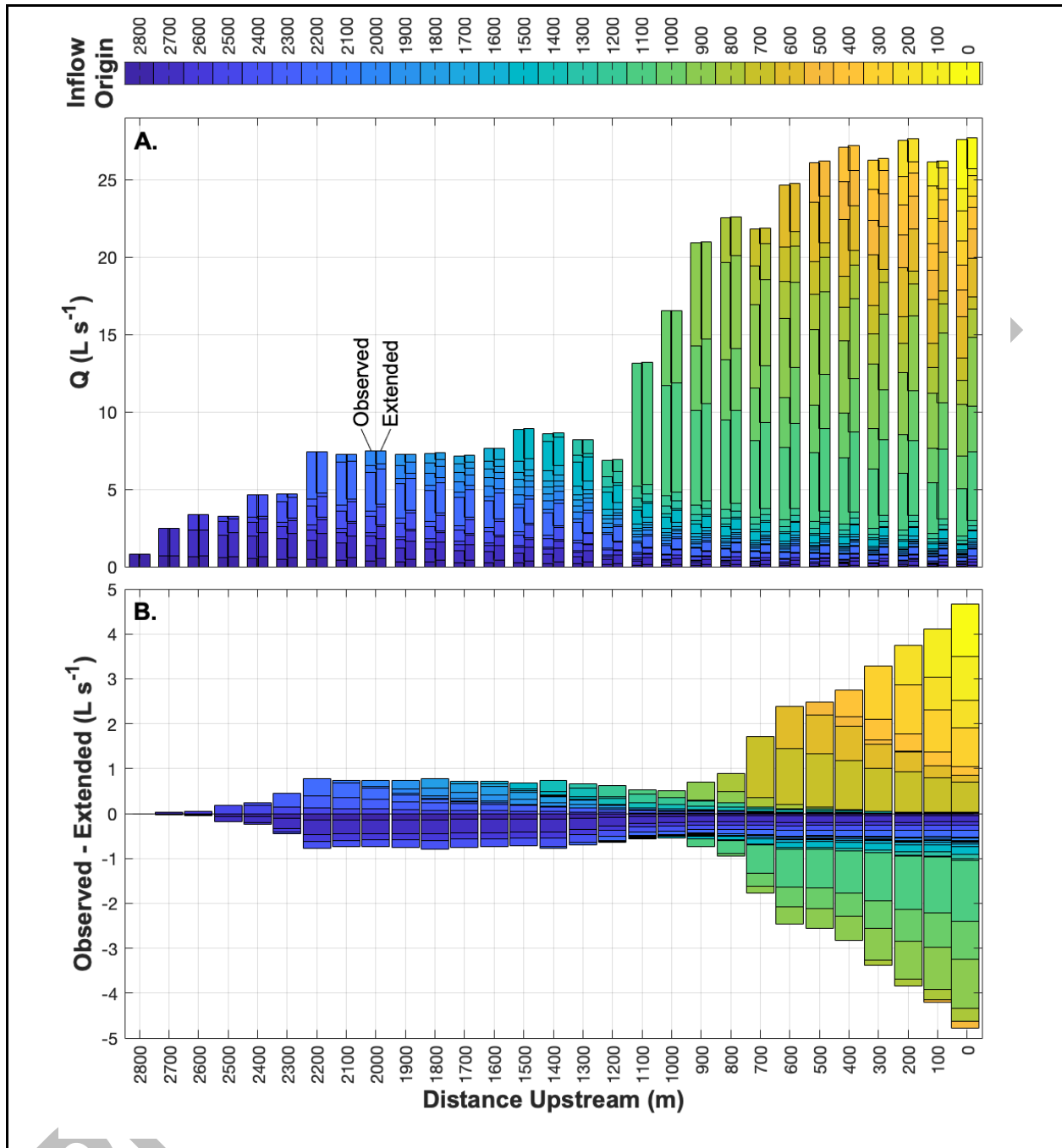


Fig. 5. (A) Channel water composition for each segment based on the location of gross gains where water entered the channel, as represented by their color. For each segment, the left stack of bars is derived from the observed mass recoveries, while the right stack includes the marginal mass recoveries. The height of each bar within a 'stack' denotes the discharge originating from a given spatial location. While overall patterns are visually similar, differences within the bars show the impact of marginal mass recovery. (B) Differences between the observed and extended mass recoveries for each segment. Values above zero indicate observed values over-estimate contributions, while negative indicate observed values under-estimate contributions to discharge.



409  
410  
411  
412  
413  
414  
415  
416  
417  
418  
419  
420  
421  
422  
423  
424  
425  
426  
427  
428  
429  
430  
431  
432  
433  
434  
435  
436  
437  
438  
439  
440  
441  
442  
443  
444  
445  
446  
447  
448  
449  
450  
451  
452  
453  
454

## 4. Discussion

### *4.1 Does marginal mass recovery change our understanding of reach- and segment-scale transport?*

Marginal mass recovery will be most important for studies concerned with the fate of all water along all timescales in a study domain. We found the marginal mass recovery (average 4.3% of total tracer) represents an average of 26% of mass that was otherwise lost to unknown fates (i.e., our ‘black box’ in the introduction). In other words, 26% of mass that was previously lost can now be attributed to flowpaths with timescales that are longer than the 100-m window of detection but shorter than the 200-m window of detection. Thus, not only can more mass be explained, but it can be assigned to a particular subset of storage timescales. Additionally, the mass that remains lost can now be confidently assigned to timescales longer than the WoD for the 200-m reach. For studies whose primary objective is to characterize the stream transport processes of advection and longitudinal dispersion, marginal mass recovery is likely inconsequential, as such studies have been a cornerstone of research for decades and not apparently suffered due to relatively small mass losses (Fischer, 1979). However, for studies attempting to allocate the age composition of catchment outflows (Harman et al., 2016; Ward et al., 2019; Ward, Kurz, et al., 2019a), marginal mass recovery informs a previously unobserved suite of timescales.

Beyond timescales and ages of water, the flowpaths associated with marginal mass recovery may also impact our interpretations of biogeochemical functioning of study reaches. The biogeochemical importance of flowpaths associated with marginal mass recovery will depend on the timescale of these flowpaths in comparison to the timescale of the process of interest. For example, nitrification is a relatively rapid process, so we might expect that nitrification reactions would be substantially completed along all flowpaths within the 100-m WoD. In that case, a 4.3% increase in the marginal mass recovery would increase the estimated amount of nitrification by 4.3%. Generalizing, for rapid processes (instantaneous transformation at the downwelling location being the extreme), marginal mass recovery will be directly proportional to our inferred amount of transformations occurring in a reach. In this case (where function is biased toward the head of the flowpath), marginal mass recovery will yield a directly proportional increase in realized function per unit of marginal mass recovered. In contrast, consider a typically-slower process like denitrification. For bulk denitrification to occur, extensive anaerobic conditions must be present, and in many systems the consumption of dissolved oxygen can be slow. Thus, we would expect denitrification to occur preferentially at the distal ends of longer residence time flow paths. By expanding the window of detection to include longer flowpaths, we disproportionately add flowpaths that are longer, and more likely to have active denitrification, to the population of flowpaths we are interpreting. In this case (where function is biased toward longer flowpaths), marginal mass recovery will yield a disproportionately large increase in a function per unit of marginal mass recovered.

That we see substantial and variable marginal mass recovery along the study segment suggests that this change is hydrologically relevant, particularly to our ability to extend reach-scale results to estimate turnover for segments or even river networks. One common strategy to upscaling in river corridors is to represent the river as a series of shorter reaches and then route water and solutes through those reaches in series to represent segments and networks (Covino et al., 2011;

455 Gomez-Velez et al., 2015; Gomez-Velez & Harvey, 2014; Kiel & Cardenas, 2014; Mallard et al.,  
456 2014). These approaches rely upon the assumption that the processes controlling transport,  
457 transformation, or loss do not change as the spatial scale of interest grows. Put another way, we  
458 commonly assume the dominant processes measured at one scale can be directly aggregated  
459 along the network to represent larger spatial scales without any other processes emerging as  
460 important. However, our findings here document that segment-scale results are directly related to  
461 the scale of a study that is chosen, consistent with Schmadel et al. (2016). Indeed, we show that  
462 even our marginal mass recovery may have a substantial impact on the inferred composition of  
463 water along a river segment (Fig. 5). Thus, turnover interpreted directly from empirical studies  
464 presents a case of maximum plausible turnover, which has the result of minimizing the  
465 persistence of upstream contribution and amplifying the proportion of downstream contributions  
466 to streamflow. The longer the window of detection can be extended, and marginal mass recovery  
467 increased, the more persistent upstream inflows will be along a gaining river corridor.

468

#### 469 **4.2 Past advances and future directions for stream solute tracer studies**

470 The window of detection has fundamentally defined the way solute tracer studies are interpreted  
471 for more than 50 years. Early work focused on the recovered solute tracer, including  
472 measurement of advective and dispersive processes and the study of mixing zones (e.g., Fischer,  
473 1979; Fig. 6A). Comparisons of mass recovery were the basis to assess net gains of stream water  
474 via dilution or used to inform losses of reactive compounds (e.g., Newbold et al., 1981). The  
475 observed time series (Fig. 6B), rather than the total masses, are the basis for studies using the  
476 popular transient storage model (Bencala & Walters, 1983; Knapp & Kelleher, 2020; Runkel,  
477 1998), and a host of other modeling approaches (Haggerty & Reeves, 2002; Rathore et al., 2021;  
478 Worman et al., 2002) and empirical calculations (Covino et al., 2010). Still, these advances came  
479 with the often unstated recognition that the empirical data themselves were subject to limitation  
480 (J. W. Harvey et al., 1996; Wagner & Harvey, 1997). The interpretation of tracer mass beyond  
481 the window of detection has, too, been the subject of inquiry. For example, Payn et al. (2009)  
482 implemented a channel water balance, building upon concepts outlined by Harvey et al. (1996).  
483 Most recently, partitioning recovered mass into that which is primarily associated with advection  
484 and dispersion from that which is primarily associated with transient storage further subdivide  
485 recovered mass based on process domain (Mason et al., 2012; Wlostowski et al., 2017; Fig. 6D).

486

487 In this study we pioneer the interpretation of co-located studies with different WoDs to define  
488 and characterize a suite of intermediate timescale flowpaths (Fig. 6E). Using our experimental  
489 design, we are now able to divide formerly lost mass into that which is recovered in a marginally  
490 longer WoD ( $M_{\text{marg}}$ ). Ultimately we are creating another ‘bin’ of timescales and associated solute  
491 masses that extend our interpretations in time (Fig. 6E). All prior approaches (Fig. 6A-6D) are  
492 still valid and appropriate, and we admittedly still cannot precisely account for the fate of all  
493 unrecovered mass (e.g., we cannot differentiate between all classes of flowpaths in Fig. 1). Still,  
494 this advance demonstrates that by manipulating the experimental design of a solute tracer study -  
495 in this case considering both 100- and 200-m segments - enables interpretation of flowpaths that  
496 would not have been considered if only conducting studies at a fixed length. Moreover, this  
497 experimental design is not limited to two overlapping segments as we considered here. This  
498 approach could be readily extended to consider a series of increasingly longer, overlapping study  
499 segments that would enable further resolution at timescales beyond the traditional WoD (Fig. 6F)  
500 until practical detection limitations are reached for a given solute tracer.

501  
502 For future studies, especially those that will use empirical data as a basis for estimation of  
503 network turnover along segments or networks (after Covino et al., 2011; Mallard et al., 2014),  
504 we recommend that assessment of marginal mass recovery is conducted. This could be  
505 implemented through multiple overlapping reaches (as implemented here), by releasing different  
506 masses or types of tracer to extend detection limits for a fixed study segment, or using  
507 instruments of varied detection limits in a single reach. Most importantly, we also emphasize  
508 here that spatially longer study reaches will necessarily capture temporally longer flowpaths, so  
509 increased study reach length is recommended as a general strategy. For studies where channel  
510 water balance and subsequent network turnover are not the focus, assessment of marginal mass  
511 losses may still offer some benefit. For example, while it does not definitively account for the  
512 fate of all mass, our approach does generate a realistic range of plausible mass recoveries that  
513 provide some estimate beyond the traditional WoD. This allows for a range of plausible  
514 segment-scale calculations to be generated, acknowledging the inherent uncertainties in selecting  
515 study segments instead of taking the WoD as a fixed limitation that must be ‘worked around’  
516 instead of ‘worked with’.

#### 517 518 ***4.3 Outstanding uncertainties and propagation of error in scaling***

519 We contend that marginal mass recovery provides useful reach-scale information about a solute  
520 tracer study and how to interpret results, but emphasize here that this strategy does not yield  
521 complete understanding of reaches and their exchanges. Marginal mass recovery, as  
522 implemented here, enables researchers to ask ‘What would be different if my study designs were  
523 incrementally different?’ and assess the sensitivity of their perceptual models or quantitative  
524 predictions to marginal changes at the limits of empirical detection. Still, other sources of error  
525 will persist including measurement of tracer masses, equipment calibration, incomplete mixing  
526 in streams, and assumptions that a sensor- or sample-based measurement occurs in a  
527 representative location in the cross-section of a stream or river. Perhaps most importantly, stream  
528 discharge is a critical variable in channel water balance and mass recovery estimates. Error in  
529 discharge measurements (due to any of the previously cited potential sources of error if dilution  
530 gauging is used) will have a directly proportional impact on inferred mass recovery. Thus, in  
531 addition to assessment of marginal mass recovery, we strongly recommend additional care is  
532 given to calculation of discharge. This could be realized by making discharge measurements  
533 independently of the tracer (e.g., via velocity gauging or co-location a station with an established  
534 stream gauge), building a stage-discharge relationship from several replication dilution gauging  
535 experiments, using multiple in-stream sensors to validate complete mixing (e.g., Clow &  
536 Fleming, 2008), or otherwise assessing uncertainty in discharge and propagating that through  
537 calculations (Emmanuelson et al., n.d.; Ward et al., 2019).

538  
539 Beyond error at the reach scale, our analysis highlights the potentially compounding and  
540 propagating of error that is possible as we represent segments and networks as a series of reaches  
541 operating in serial (as in Covino et al., 2011; Gomez-Velez & Harvey, 2014; J. Harvey et al.,  
542 2019b; Kiel & Cardenas, 2014). Indeed, this representation of segments requires several  
543 assumptions that are not always explicitly stated nor justified. First, the approach requires that  
544 the reach-scale experiments are, themselves, an appropriate scale to characterize the most  
545 important processes. In the case of hyporheic exchange, one practical consequence is assuming  
546 that unmeasured flowpaths beyond are within the window of detection are unimportant. Next, the

547 approach requires that the processes that are integrated by the recovered tracer at the reach-scale  
548 are characterized by the empirical data. Put another way, the reach itself must be a representative  
549 sampling of the processes that are important. This has been assumed by fixing study reach  
550 lengths (as in this study & Schmadel et al., 2016), advective timescales (e.g., Ward et al., 2019),  
551 establishing a standardized length-scale (Runkel, 2002), or assuming that a scale established by  
552 one discipline will be relevant for another (e.g., 20 wetted channel widths as a reach-scale from  
553 geomorphologists as a basis for planning solute tracer studies; Ward et al., 2019, 2019). To our  
554 knowledge, none of these assumptions has been explicitly tested in the field for solute tracer  
555 studies. Finally, this approach assumes that no new controls will emerge as important as spatial  
556 scales are increased.  
557

PRE-REVIEW DRAFT

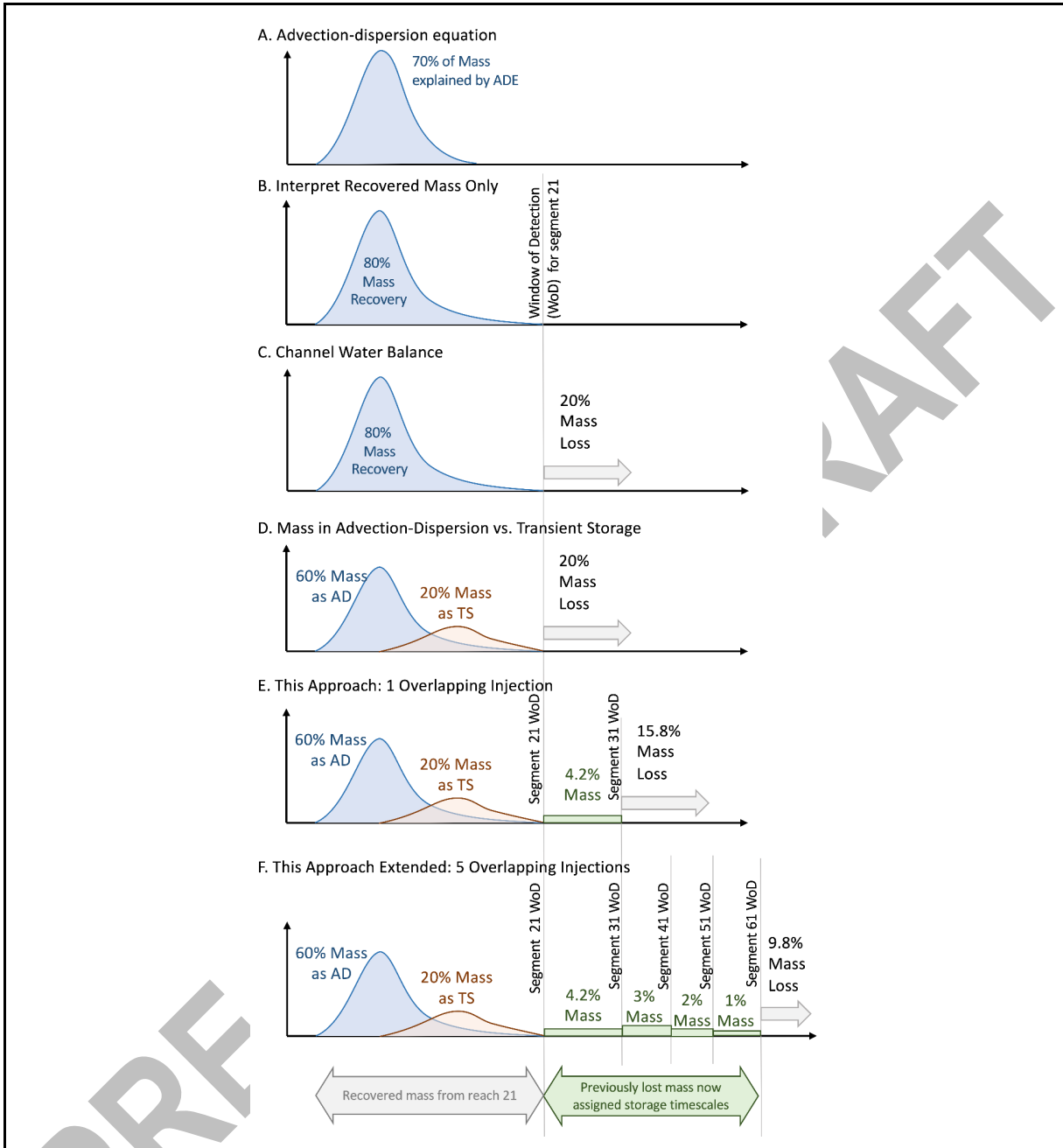


Fig. 6. Evolving interpretation of stream solute tracer studies in the past 50 years. Tracer studies were initially used to estimate mixing and dispersion (A), and later transient storage (B). More recent work has extended interpretations to channel water balance (C) and partitioning recovered tracer into fractions with dominant transport by transient storage (D). In this study, we demonstrate manipulation of the window of detection to further assign mass to a range of timescales (E), which could be readily extended with increasingly long reaches and/or sensitivity to different tracers (F). In all cases, the quantitative values provided are intended as illustrative, relative values and not presenting any specific data set.

560

## 561 **5. Conclusions**

562 Our overarching goal in this manuscript was to ask if and how marginally extended the window  
563 of detection, and thereby extended empirical mass recovery to a broader suite of flowpaths,  
564 would change our understanding of reach- and segment-scale transport in river corridors. We  
565 found that shorter (100-m) reaches did not systematically bias toward more or less mass recovery  
566 than the 200-m reaches they were located within. Marginal mass recovery was able to explain an  
567 average of about 26% of lost tracer mass, representing an average of 4.3% of total solute tracer  
568 mass (range 1.3-10.1%) across our replicates. This change in mass recovery was important, as  
569 we found representing a 200-m reach as a series of 2x100-m reaches systematically  
570 underestimate mass recovery. Consequently, studies without marginal mass recovery  
571 overestimated magnitudes of gross gains and losses in the marginally longer 200-m reaches in all  
572 cases. Moreover, this bias was amplified when we represented segments as a series of reaches,  
573 leading to interpretations that underestimated the persistence of distal segments and  
574 overestimated the importance of gains occurring near the catchment outlet.

575

576 Ultimately, some amount of solute mass loss to unknown fates is to be expected in any solute  
577 tracer study given detection limits and complex, multi-scale flowpath networks. Thus, we  
578 suggest that researchers embrace the window of detection, taking advantage of experimental  
579 design to assess marginal mass recovery. This provides context for interpretation of empirical  
580 data, yielding a quantitative basis for assessment of uncertainty associated with detection limits.  
581 Moreover, if tracers, sensitivities, or experimental designs are planned appropriately, marginal  
582 mass recovery could be used to systematically probe flowpaths with longer duration (e.g., Fig.  
583 6F), informing transport at previously unobserved timescales.

584

585 Finally, the use of reach-scale understanding as a basis for representation of segments (as a series  
586 of reaches) or network (as a series of segments) is being used as one basis to make predictions at  
587 large spatial scales (e.g., Covino et al., 2011; Gomez-Velez et al., 2015; Kiel & Cardenas, 2014).  
588 However, we encourage caution in aggregating reaches to represent segments and network, as  
589 this implicitly assumes (1) that reach-scale results are complete in their representation of  
590 timescales and processes; (2) reach-scale results appropriate integrate all smaller-scale controls  
591 relevant for the process(es) of interest; and (3) no new controls emerge at larger spatial scales  
592 that would not be apparent in reach-scale studies. On balance, we expect that short reach-scale  
593 studies will truncate more of the true, underlying transit time distribution and exacerbate errors  
594 associated with scaling.

595

596

## 597 **Acknowledgements**

598 The initial data collection was research was supported by collaborative NSF awards EAR  
599 0337650 and EAR 0530873. We thank the Tenderfoot Creek Experimental Forest and the U.S.  
600 Department of Agriculture for support of field research at the site. We thank Ken Bencala for  
601 input on early versions of this study and continued mentoring. Ward led the data analysis and  
602 writing of this manuscript, with input and support from all coauthors. Ward was support in part  
603 by Department of Energy awards DE-SC000022 and DE-SC0019377. Ward's time was  
604 supported in part by NSF Award EAR 1652293, the Burnell and Barbara Fischer fellowship  
605 from Indiana University, sabbatical support from J. Selker and Oregon State University, and the

606 the Fulbright – University of Birmingham Scholar program. Any views or opinions expressed in  
607 this study are those of the authors and not positions of their employers.

608

#### 609 **Data Availability**

610 Data are available in Payn and Ward (2022).

611

#### 612 **References**

613 Alexander, R. B., Böhlke, J. K., Boyer, E. W., David, M. B., Harvey, J. W., Mulholland, P. J., et al.  
614 (2009). Dynamic modeling of nitrogen losses in river networks unravels the coupled  
615 effects of hydrological and biogeochemical processes. *Biogeochemistry*, 93(1–2), 91–116.  
616 <https://doi.org/10.1007/S10533-008-9274-8/FIGURES/7>

617 Bencala, K. E. (1983). Simulation of Solute Transport in a Mountain Pool-and-Riffle Stream  
618 With a Kinetic Mass Transfer Model for Sorption. *Water Resources Research*, 19(3), 732–  
619 738. <https://doi.org/10.1029/WR019i003p00732>

620 Bencala, K. E., & Walters, R. A. (1983). Simulation of solute transport in a mountain pool-and-  
621 riffle stream: a transient storage model. *Water Resources Research*, 19(3), 718–724.  
622 <https://doi.org/10.1029/WR019i003p00718>

623 Bencala, K. E., Kennedy, V. C., Zellweger, G. W., & Jackman, A. P. (1984). An Experimental  
624 Analysis of Cation and Anion Transport, 20(12), 1797–1803.

625 Briggs, M. A., Gooseff, M. N., Arp, C. D., & Baker, M. A. (2009). A method for estimating  
626 surface transient storage parameters for streams with concurrent hyporheic storage. *Water*  
627 *Resources Research*.

628 Cirpka, O. A., Fienen, M. N., Hofer, M., Hoehn, E., Tessarini, A., Kipfer, R., & Kitanidis, P. K.  
629 (2007). Analyzing bank filtration by deconvoluting time series of electric conductivity.  
630 *Ground Water*, 45(3), 318–328.

631 Clow, D. W., & Fleming, A. C. (2008). Tracer gauge: An automated dye dilution gauging system  
632 for ice-affected streams. *Water Resources Research*, 44(12).  
633 <https://doi.org/10.1029/2008WR007090>

634 Covino, T. P., McGlynn, B. L., & McNamara, R. a. (2010). Tracer Additions for Spiraling Curve  
635 Characterization (TASCC): Quantifying stream nutrient uptake kinetics from ambient to  
636 saturation. *Limnology and Oceanography: Methods*, 8, 484–498.  
637 <https://doi.org/10.4319/lom.2010.8.484>

638 Covino, T. P., McGlynn, B. L., & Mallard, J. (2011). Stream-groundwater exchange and  
639 hydrologic turnover at the network scale. *Water Resources Research*, 47(12), W12521.

640 Drummond, J. D., Covino, T. P., Aubeneau, a. F., Leong, D., Patil, S., Schumer, R., & Packman,  
641 A. I. (2012). Effects of solute breakthrough curve tail truncation on residence time  
642 estimates: A synthesis of solute tracer injection studies. *Journal of Geophysical Research:*  
643 *Biogeosciences*, 117(3), 1–11. <https://doi.org/10.1029/2012JG002019>

644 Emmanuelson, K., Covino, T. P., Ward, A. S., Dorley, J., & Gooseff, M. N. (n.d.). Conservative  
645 solute transport processes and associated transient storage mechanisms: Comparing streams  
646 with contrasting channel morphologies, land use, and land cover. *Hydrological Processes*.  
647 Retrieved from <https://ejournal3.undip.ac.id/index.php/jamt/article/view/5101>

648 Fischer, H. B. (1979). *Mixing in inland and coastal waters*. Academic Pr.

649 Frissell, C. A., Liss, W. J., Warren, C. E., & Hurley, M. D. (1986). A hierarchical framework for  
650 stream habitat classification: Viewing streams in a watershed context. *Environmental*  
651 *Management*, 10(2), 199–214.

- 652 Fuller, C. C., & Harvey, J. W. (2000). Reactive uptake of trace metals in the hyporheic zone of a  
653 mining-contaminated stream, Pinal Creek, Arizona. *Environmental Science & Technology*,  
654 34(7), 1150–1155.
- 655 Gomez-Velez, J. D., & Harvey, J. W. (2014). A hydrogeomorphic river network model predicts  
656 where and why hyporheic exchange is important in large basins. *Geophysical Research*  
657 *Letters*, 41, 6403–6412. <https://doi.org/doi:10.1002/2014GL061099>
- 658 Gomez-Velez, J. D., Harvey, J. W., Cardenas, M. B., & Kiel, B. (2015). Denitrification in the  
659 Mississippi River network controlled by flow through river bedforms. *Nature Geoscience*,  
660 8(October), 1–8. <https://doi.org/10.1038/ngeo2567>
- 661 Gooseff, M. N., McKnight, D. M., Runkel, R. L., & Vaughan, B. H. (2003). Determining long  
662 time-scale hyporheic zone flow paths in Antarctic streams. *HYDROLOGICAL*  
663 *PROCESSES*, 17(9), 1691–1710. Retrieved from  
664 [http://getit.libraries.psu.edu:9003/sfx\\_local?url\\_ver=Z39.88-  
665 2004&url\\_ctx\\_fmt=info:ofi/fmt:kev:mtx:ctx&rft\\_val\\_fmt=info:ofi/fmt:kev:mtx:journal&rft.  
666 atitle=Determining long time-scale hyporheic zone flow paths in Antarctic  
667 streams&rft.auinit=M&rft.aulast=G](http://getit.libraries.psu.edu:9003/sfx_local?url_ver=Z39.88-2004&url_ctx_fmt=info:ofi/fmt:kev:mtx:ctx&rft_val_fmt=info:ofi/fmt:kev:mtx:journal&rft.atitle=Determining%20long%20time-scale%20hyporheic%20zone%20flow%20paths%20in%20Antarctic%20streams&rft.auinit=M&rft.aulast=G)
- 668 Guillet, G., Knapp, J. L. A., Merel, S., Cirpka, O. A., Grathwohl, P., Zwiener, C., & Schwientek,  
669 M. (2019). Fate of wastewater contaminants in rivers: Using conservative-tracer based  
670 transfer functions to assess reactive transport. *Science of The Total Environment*, 656,  
671 1250–1260. <https://doi.org/10.1016/J.SCITOTENV.2018.11.379>
- 672 Haggerty, R., & Reeves, P. (2002). STAMMT-L Version 1.0 User's Manual. *Sandia National*  
673 *Laboratories [ERMS# 520308]*, 1–76.
- 674 Haggerty, R., Wondzell, S. M., & Johnson, M. A. (2002). Power-law residence time distribution  
675 in the hyporheic zone of a 2nd-order mountain stream. *Geophysical Research Letters*,  
676 29(13), 1640.
- 677 Harman, C. J., Ward, A. S., & Ball, A. (2016). How does reach-scale stream-hyporheic transport  
678 vary with discharge? Insights from SAS analysis of sequential tracer injections in a  
679 headwater mountain stream. *Water Resources Research*, 52, 7130–7150.  
680 <https://doi.org/10.1002/2016WR018832>.Received
- 681 Harvey, J., Gomez-Velez, J., Schmadel, N. M., Scott, D., Boyer, E. W., Alexander, R. B., et al.  
682 (2019a). How Hydrologic Connectivity Regulates Water Quality in River Corridors.  
683 *Journal of the American Water Resources Association*, 55(2), 369–381.  
684 <https://doi.org/10.1111/1752-1688.12691>
- 685 Harvey, J., Gomez-Velez, J., Schmadel, N., Scott, D., Boyer, E., Alexander, R., et al. (2019b).  
686 How Hydrologic Connectivity Regulates Water Quality in River Corridors. *JAWRA Journal*  
687 *of the American Water Resources Association*, 55(2), 369–381.  
688 <https://doi.org/10.1111/1752-1688.12691>
- 689 Harvey, J. W., & Fuller, C. C. (1998). Effect of enhanced manganese oxidation in the hyporheic  
690 zone on basin-scale geochemical mass balance. *Water Resources Research*, 34(4), 623–636.
- 691 Harvey, J. W., & Wagner, B. J. (2000). Quantifying hydrologic interactions between streams and  
692 their subsurface hyporheic zones. In J. B. Jones & P. J. Mulholland (Eds.), *Streams and*  
693 *Ground Waters* (pp. 3–44).
- 694 Harvey, J. W., Wagner, B. J., & Bencala, K. E. (1996). Evaluating the reliability of the stream  
695 tracer approach to characterize stream-subsurface water exchange. *Water Resources*  
696 *Research*, 32(8), 2441–2451.
- 697 Herzog, S. P., Ward, A. S., & Wondzell, S. M. (2019). Multiscale Feature-feature Interactions



698 Control Patterns of Hyporheic Exchange in a Simulated Headwater Mountain Stream.  
699 *Water Resources Research*, 1–17. <https://doi.org/10.1029/2019WR025763>

700 Jackman, A. P., Walters, R. A., & Kennedy, V. C. (1984). Transport and concentration controls  
701 for chloride, strontium, potassium and lead in Uvas Creek, a small cobble-bed stream in  
702 Santa Clara County, California, U.S.A.: 2. Mathematical modeling. *Journal of Hydrology*,  
703 75(1–4), 111–141.

704 Jackson, T. R., Haggerty, R., Apte, S. V., Coleman, A., & Drost, K. J. (2012). Defining and  
705 measuring the mean residence time of lateral surface transient storage zones in small  
706 streams. *Water Resources Research*, 48(10), 1–20. <https://doi.org/10.1029/2012WR012096>

707 Jackson, T. R., Haggerty, R., Apte, S. V., & O’Connor, B. L. (2013). A mean residence time  
708 relationship for lateral cavities in gravel-bed rivers and streams: Incorporating streambed  
709 roughness and cavity shape. *Water Resources Research*, 49(6), 3642–3650.  
710 <https://doi.org/10.1002/wrcr.20272>

711 Karwan, D. L., & Saiers, J. E. (2009). Influences of seasonal flow regime on the fate and  
712 transport of fine particles and a dissolved solute in a New England stream. *Water Resources*  
713 *Research*, 45(11), W11423.

714 Keefe, S. H., Barber, L. B., Runkel, R. L., Ryan, J. N., Mcknight, D. M., Wass, R. D., et al.  
715 (2004). Conservative and reactive solute transport in constructed wetlands. *Water Resources*  
716 *Research*, 40(1), 1201. <https://doi.org/10.1029/2003WR002130>

717 Kelleher, C. A., Wagener, T., McGlynn, B. L., Ward, A. S., Gooseff, M. N., & Payn, R. A.  
718 (2013). Identifiability of transient storage model parameters along a mountain stream.  
719 *Water Resources Research*, 49(9), 5290–5306. <https://doi.org/10.1002/wrcr.20413>

720 Kiel, B., & Cardenas, M. (2014). Lateral hyporheic exchange throughout the Mississippi River  
721 network. *Nature Geoscience*, 7(May), 413–417. <https://doi.org/10.1038/ngeo2157>

722 Klockner, C. A., Kaushal, S. S., Groffman, P. M., Mayer, P. M., & Morgan, R. P. (2009).  
723 Nitrogen uptake and denitrification in restored and unrestored streams in urban Maryland,  
724 USA. *Aquatic Sciences-Research Across Boundaries*, 71(4), 411–424.

725 Knapp, J. L. A., & Kelleher, C. (2020). A Perspective on the Future of Transient Storage  
726 Modeling: Let’s Stop Chasing Our Tails. *Water Resources Research*, 56(3),  
727 e2019WR026257. <https://doi.org/10.1029/2019WR026257>

728 Knust, A. E., Warwoel, J. J., & Warwick, J. J. (2009). Using a fluctuating tracer to estimate  
729 hyporheic exchange in restored and unrestored reaches of the Truckee River, Nevada, USA.  
730 *HYDROLOGICAL PROCESSES*, 23(8), 1119–1130. Retrieved from  
731 <http://dx.doi.org/10.1002/hyp.7218>

732 Lamontagne, S., & Cook, P. G. (2007). Estimation of hyporheic water residence time in situ  
733 using <sup>222</sup>Rn disequilibrium. *Limnology and Oceanography: Methods*, 5(11), 407–416.  
734 <https://doi.org/10.4319/LOM.2007.5.407>

735 Lange, J., Schuetz, T., Gregoire, C., Elsässer, D., Schulz, R., Passeur, E., & Tournebize, J.  
736 (2011). Multi-tracer experiments to characterise contaminant mitigation capacities for  
737 different types of artificial wetlands. <https://doi.org/10.1080/03067319.2010.525635>,  
738 91(7–8), 768–785. <https://doi.org/10.1080/03067319.2010.525635>

739 Larson, L. N., Fitzgerald, M., Singha, K., Gooseff, M. N., Macalady, J. L., & Burgos, W. (2013).  
740 Hydrogeochemical niches associated with hyporheic exchange beneath an acid mine  
741 drainage-contaminated stream. *Journal of Hydrology*, 501, 163–174.  
742 <https://doi.org/10.1016/j.jhydrol.2013.08.007>

743 Mallard, J., McGlynn, B. L., & Covino, T. P. (2014). Lateral inflows, stream-groundwater

744 exchange, and network geometry influence streamwater composition. *Water Resources*  
745 *Research*, 50, 4603–4623. <https://doi.org/10.1002/2013WR014222>. Received  
746 Mason, S. J. K., McGlynn, B. L., & Poole, G. C. (2012). Hydrologic response to channel  
747 reconfiguration on Silver Bow Creek, Montana. *Journal of Hydrology*, 438–439, 125–136.  
748 Mulholland, P. J., Helton, A. M., Poole, G. C., Hall, R. O., Hamilton, S. K., Peterson, B. J., et al.  
749 (2008). Stream denitrification across biomes and its response to anthropogenic nitrate  
750 loading. *Nature*, 452(7184), 202–5. <https://doi.org/10.1038/nature06686>  
751 Newbold, J. D., Elwood, J. W., O’Neill, R. V., & Van Winkle, W. (1981). Measuring Nutrient  
752 Spiraling in Streams. *Canadian Geotechnical Journal*, 38, 860–863.  
753 Ninnemann, J. J. (2005). *A study of hyporheic characteristics along a longitudinal profile of*  
754 *Lookout Creek, Oregon*. Oregon State University.  
755 <https://doi.org/10.1017/CBO9781107415324.004>  
756 Patil, S., Covino, T. P., Packman, A. I., McGlynn, B. L., Drummond, J. D., Payn, R. A., &  
757 Schumer, R. (2013). Instream variability in solute transport: Hydrologic and geomorphic  
758 controls on solute retention. *Journal of Geophysical Research: Earth Surface*, 118(2), 413–  
759 422. <https://doi.org/10.1029/2012JF002455>  
760 Payn, R. A., & Ward, A. S. (2022). Solute tracer timeseries, Stringer Creek, 2005 and 2006.  
761 Retrieved April 4, 2022, from  
762 <http://www.hydroshare.org/resource/efb41192ddbd4785a2b0ef00bf5e7c62>  
763 Payn, R. A., Gooseff, M. N., McGlynn, B. L., Bencala, K. E., & Wondzell, S. M. (2009).  
764 Channel water balance and exchange with subsurface flow along a mountain headwater  
765 stream in Montana, United States. *Water Resources Research*, 45.  
766 Rathore, S. S., Jan, A., Coon, E. T., & Painter, S. L. (2021). On the Reliability of Parameter  
767 Inferences in a Multiscale Model for Transport in Stream Corridors. *Water Resources*  
768 *Research*, 57(5), e2020WR028908. <https://doi.org/10.1029/2020WR028908>  
769 Runkel, R. L. (1998). *One-dimensional Transport with Inflow and Storage (OTIS): A Solute*  
770 *Transport Model for Streams and Rivers*. Director. US Dept. of the Interior, US Geological  
771 Survey; Information Services [distributor]. [https://doi.org/Cited By \(since 1996\) 47\nExport](https://doi.org/Cited%20By%20(since%201996)%2047%20Export%20Date%204%20April%202012)  
772 Date 4 April 2012  
773 Runkel, R. L. (2002). A new metric for determining the importance of transient storage. *Journal*  
774 *of the North American Benthological Society*, 21(4), 529–543.  
775 Schmadel, N. M., Ward, A. S., Kurz, M. J., Fleckenstein, J. H., Zarnetske, J. P., Knapp, J. L. A.,  
776 et al. (2016). Stream solute tracer timescales changing with discharge and reach length  
777 confound process interpretation. *Water Resources Research*, 52, 3227–3245.  
778 <https://doi.org/10.1002/2015WR018062>. Received  
779 Stream Solute Workshop. (1990). Concepts and Methods for Assessing Solute Dynamics in  
780 Stream Ecosystems. *Journal of the North American Benthological Society*, 9(2), 95–119.  
781 Retrieved from <http://www.jstor.org/stable/1467445>  
782 Tank, J. L., Rosi-Marshall, E. J., Baker, M. A., & Hall, R. O. (2008). Are rivers just big streams?  
783 A pulse method to quantify nitrogen demand in a large river. *Ecology*, 89(10), 2935–2945.  
784 Toth, J. (1962). A theory of groundwater motion in small drainage basins in central Alberta,  
785 Canada. *Journal of Geophysical Research*, 67(11), 4375–4387.  
786 Tóth, J. (1963). A theoretical analysis of groundwater flow in small drainage basins. *Journal of*  
787 *Geophysical Research*, 68(16), 4795–4812. <https://doi.org/10.1029/JZ068i016p04795>  
788 Wagner, B. J., & Harvey, J. W. (1997). Experimental design for estimating parameters of rate-  
789 limited mass transfer: Analysis of stream tracer studies. *Water Resources Research*, 33(7),

790 1731–1741.

791 Ward, A. S., Fitzgerald, M., Gooseff, M. N., Voltz, T. J., Binley, A. M., & Singha, K. (2012).  
792 Hydrologic and geomorphic controls on hyporheic exchange during base flow recession in a  
793 headwater mountain stream. *Water Resources Research*, 48(4), W04513.

794 Ward, A. S., Gooseff, M. N., Voltz, T. J., Fitzgerald, M., Singha, K., & Zarnetske, J. P. (2013).  
795 How does rapidly changing discharge during storm events affect transient storage and  
796 channel water balance in a headwater mountain stream? *Water Resources Research*, 49(9),  
797 5473–5486. <https://doi.org/10.1002/wrcr.20434>

798 Ward, A. S., Kelleher, C. A., Mason, S. J. K., & Wagener, T. (2016). A software tool to assess  
799 uncertainty in transient-storage model parameters using Monte Carlo simulations.  
800 *Freshwater Science*, 36(December 2016). <https://doi.org/10.1086/690444>.

801 Ward, A. S., Morgan, J. A., White, J. R., & Royer, T. V. (2018). Streambed restoration to  
802 remove fine sediment alters reach-scale transient storage in a low-gradient 5th order river,  
803 Indiana, USA. *Hydrological Processes*, 1–15. <https://doi.org/10.1002/hyp.11518>

804 Ward, A. S., Zarnetske, J. P., Baranov, V., Blaen, P. J., Brekenfeld, N., Chu, R., et al. (2019).  
805 Co-located contemporaneous mapping of morphological, hydrological, chemical, and  
806 biological conditions in a 5th-order mountain stream network, Oregon, USA. *Earth System  
807 Science Data*, 11(4). <https://doi.org/10.5194/essd-11-1567-2019>

808 Ward, A. S., Kurz, M. J., Schmadel, N. M., Knapp, J. L. A., Blaen, P. J., Harman, C. J., et al.  
809 (2019a). Solute transport and transformation in an intermittent, headwater mountain stream  
810 with diurnal discharge fluctuations. *Water (Switzerland)*, 11(11).  
811 <https://doi.org/10.3390/w11112208>

812 Ward, A. S., Kurz, M. J., Schmadel, N. M., Knapp, J. L. A., Blaen, P. J., Harman, C. J., et al.  
813 (2019b). Solute Transport and Transformation in an Intermittent, Headwater Mountain  
814 Stream with Diurnal Discharge Fluctuations. *Water 2019, Vol. 11, Page 2208, 11(11), 2208*.  
815 <https://doi.org/10.3390/W11112208>

816 Ward, A. S., Wondzell, S. M., Schmadel, N. M., Herzog, S., Zarnetske, J. P., Baranov, V., et al.  
817 (2019). Spatial and temporal variation in river corridor exchange across a 5th order  
818 mountain stream network. *Hydrology and Earth System Sciences Discussions*, (April), 1–  
819 39. <https://doi.org/10.5194/hess-2019-108>

820 Wlostowski, A. N., Gooseff, M. N., Bowden, W. B., & Wollheim, W. M. (2017). Stream tracer  
821 breakthrough curve decomposition into mass fractions: A simple framework to analyze and  
822 compare conservative solute transport processes. *Limnology and Oceanography: Methods*,  
823 15(2), 140–153. <https://doi.org/10.1002/lom3.10148>

824 Worman, A., & Wachniew, P. (2007). Reach scale and evaluation methods as limitations for  
825 transient storage properties in streams and rivers. *Water Resources Research*, 43(10), 13.  
826 <https://doi.org/10.1029/2006wr005808>

827 Worman, A., Packman, A. I., & Jonsson, K. (2002). Effect of flow-induced exchange in  
828 hyporheic zones on longitudinal transport of solutes in streams and rivers *Ha*, 38(1).  
829  
830

831 **Supplemental Information**

832 Across the entire system, the mass along each flowpath (labeled A through I in Fig. S1)  
833 can be calculated by the set of equations:

834

$$M_A = M_3$$

835

836

$$M_B = M_A f_{rec32}$$

837

838

$$M_C = M_A(1 - f_{rec32})$$

839

840

$$M_D = M_C f_{int32}$$

841

842

$$M_E = M_C(1 - f_{int32})$$

843

844

$$M_F = M_B + M_D$$

845

846

$$M_G = M_F f_{rec21}$$

847

848

$$M_H = M_F(1 - f_{rec21})$$

849

850

$$M_I = M_H f_{int21}$$

851

852

$$M_J = M_H(1 - f_{int21})$$

853

854

$$M_K = M_I + M_G$$

855

856

857 where  $M_X$  represents the total mass transported along flowpath X,  $f_{int}$  represents the fraction of  
858 mass traveling along an intermediate flowpath, and  $f_{rec}$  represent the fraction of mass recovered  
859 in the stream channel.

860

861 Using these equations, mass balance for the entire system can be expressed as:

862

863

$$M_3 = M_{rec31} + M_{loss32} + M_{loss21}$$

864

865

866

867

868

869

870

871

where  $M_{lossXY}$  represents the mass lost in study segment XY (i.e., mass not returning to the stream within the study reach, Flowpaths D and G in Fig. 1), and  $M_{rec31}$  represents the total mass recovered in the stream at the downstream end of the study segment.

If the two study segments are combined in series and assumed to have no intermediate flowpaths (i.e., no recovery of mass beyond the segment-scale window of detection),  $f_{int32} = 0$  and  $f_{int21} = 0$ ). Thus, the system outputs can be expressed as:

872  
 873  
 874  
 875  
 876  
 877  
 878  
 879  
 880  
 881  
 882  
 883  
 884  
 885  
 886  
 887  
 888  
 889  
 890

$$M_{rec31} = M_3(f_{rec32})(f_{rec21})$$

$$M_{loss32} = M_3(1 - f_{rec32})$$

$$M_{loss21} = M_3(f_{rec32})(1 - f_{rec21})$$

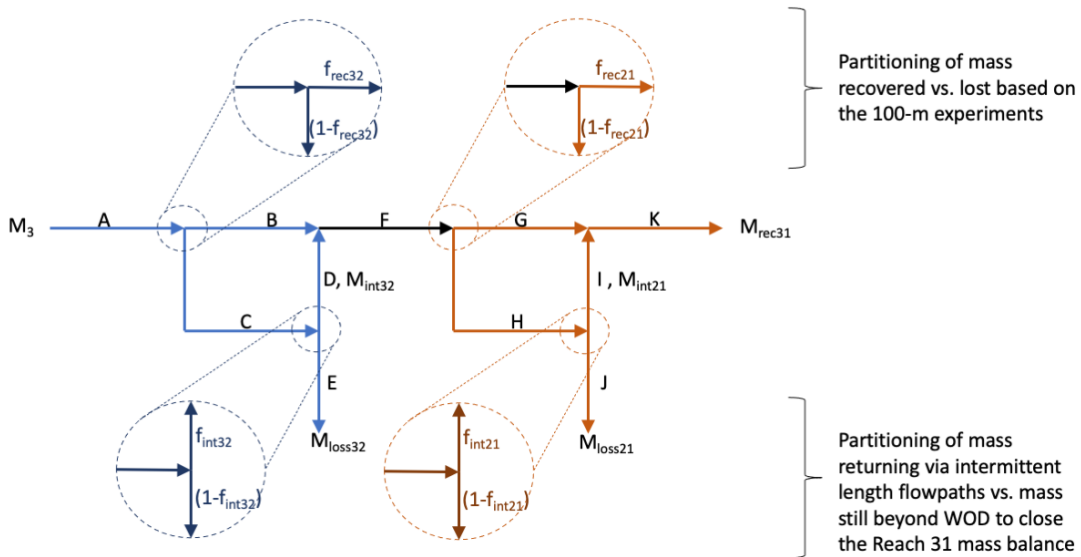
However, in the case where an extended window of detection enables detection of intermediate flowpaths (i.e.,  $f_{int32} > 0$  and  $f_{int21} > 0$ ), the system outputs become:

$$M_{rec31} = M_3[f_{rec32} + (1 - f_{rec32})f_{int32}][f_{rec21} + (1 - f_{rec21})f_{int21}]$$

$$M_{loss32} = M_3(1 - f_{rec32})(1 - f_{int32})$$

$$M_{loss21} = M_3[f_{rec32} + (1 - f_{rec32})f_{int32}](1 - f_{rec21})(1 - f_{int21})$$

where the terms in red are added due to the return of mass along intermediate flowpaths (vectors D and I in Fig. S1).



891  
 892  
 893  
 894

**Figure S1.** Mass balance used to track mass through potential flowpaths in the 200-m study system. Masses are calculated within the system at each vector (labels A-K).